Pressure-induced reentrant metallic phase in lithium

T. Matsuoka,[1,*] M. Sakata,[1] Y. Nakamoto,[1] K. Takahama,[1] K. Ichimaru,[1] K. Mukai,[1] K. Ohta,[1]
N. Hirao,[2] Y. Ohishi,[2] and K. Shimizu[1]

[1]*Center for Quantum Science and Technology under Extreme Conditions, Osaka University, Osaka 560-8531, Japan*
[2]*Japan Synchrotron Radiation Research Institute (JASRI)/SPring-8, Hyogo 679-5198, Japan*

(Received 26 December 2012; revised manuscript received 19 March 2014; published 8 April 2014)

We report the metal (0–80 GPa)–semiconductor ($oC40$, 80–120 GPa)–metal ($oC24$, >120 GPa) transitions of lithium under compression, as observed through simultaneous electrical resistance and x-ray diffraction measurements. The energy gap in the $oC40$ semiconductor quickly decreases with applied pressure, and Li reverts back to a metallic state accompanied by a structural transition to $oC24$. The large ρ value for $oC24$ indicates that this re-entrant metallic phase is a so-called "poor metal." Our results reveal a characteristic phase diagram that demonstrates the existence of a semiconductor phase between two distinct metallic phases.

DOI: 10.1103/PhysRevB.89.144103 PACS number(s): 74.62.Fj, 74.25.Dw, 74.25.F−, 74.25.Jb

Light alkali metals such as lithium (Li) and sodium (Na) play important roles in the understanding of the physical properties of metals under both ambient and high-pressure conditions. At ambient pressure, the system can be approximated using the nearly-free electron (NFE) model [1]. However, under compression, the NFE picture breaks down and the resulting anomalous physical properties have attracted significant scientific interest.

Neaton and Ashcroft predicted that pressure causes Li to undergo phase transitions to less symmetric structures. Furthermore, a metal-semiconductor transition is also induced, which is in contrast to the empirical expectations of high-pressure experiments predicting that Li becomes more free-electron-like under compression [2]. The application of pressure causes s-p orbital mixing, a strong deformation of the Fermi surface, and Jahn-Teller-like distortion [3,4]. Remarkably, theoretical calculations have demonstrated the metal-to-semiconductor transition resulting from the accumulation of electronic charge density within the interstitial region as the 2s electrons are pushed away from the atomic cores by Coulomb repulsion, Pauli exclusion, and the orthogonality of core and valence orbitals [2,5–8]. X-ray diffraction (XRD) experiments have confirmed that the structure of Li tends to transform to lower symmetry phases at high pressures (Fig. 1). In Fig. 1, apart from bcc and fcc, the phases are labeled with their structural types using the Pearson notation. Until recently, structural studies have been extended to pressures of up to 140 GPa, and the $oC24$ structure has been reported to be stable above 95 GPa and up to 140 GPa [9]. Remarkably, Li was found to be a liquid near or below room temperature even at pressures above 45 GPa [10,11]. The experimental efforts to investigate the electronic states of Li have indeed confirmed the metal's anomalous electronic properties, including superconductivity, the deviation from the NFE model, and the theoretically predicted metal-to-semiconductor transition [12–18]. Electrical resistivity has been found to increase significantly with applied pressure, indicating a deviation from the NFE model [12–14]. The superconducting transition temperature (T_c) of Li (at ambient pressure, $T_c \leqslant 0.4$ mK [15]) dramatically increases with pressure, reaching 20 K at 40 GPa [16–18], which is the second highest T_c among all elements in the periodic table [19–21]. Observation of the abrupt increase in electrical resistivity and change in temperature dependence for the $oC40$ structure has revealed that Li is a semiconductor with a very small energy gap [14]. Another example of pressure induced metal-to-semiconductor transition is for Na at above 140 GPa [22].

It has been suggested that the core-valence overlap is already large in the $oC40$ structure, and core exclusion strongly affects the behavior of valence electrons [8]. Furthermore, the importance of the zero-point energy (quantum effect) has been discussed with respect to the significant reduction in the melting point and phase stability of Li under high-pressure conditions [7,9–11].

Given these anomalous properties, it is of fundamental importance to extend the experimental studies on the electrical characteristics of Li to pressures exceeding the previously achieved value of 105 GPa [14]. Under these conditions, further enhancement in the core-valence overlap and an increased role of quantum effects are anticipated, thereby presenting the possibility for a new state of matter to be observed. Li may revert back to a metallic state with characteristic behavior arising from the strong interaction between the valence electrons and the Li-ion cores and an enhanced quantum effect. Although theoretical studies predicted the $oC24$ (*Cmca*) structure to be metallic [7,9,23–25], this has not been substantiated by experimental observations. Interestingly, the state in which core-valence overlap is strong and the quantum effect plays a dominant role in the total energy of the system is predicted for metallic hydrogen, which may exhibit behaviors such as high-temperature superconductivity and metallic superfluidity [26–28]. If Li reverts back to a metal under further compression, these experiments may serve as a step towards the realization of metallic hydrogen.

In this paper, we report on simultaneous powder XRD and electrical resistance measurements on a Li sample in a diamond anvil cell (DAC) at temperatures below 100 K and under pressures of up to 137 GPa. (XRD and electrical resistance were measured on a Li sample at the same time.) Electrical resistivity decreases by four orders of magnitude with increasing pressure at between 100 and 120 GPa,

*Present address: Department of Electrical, Electronic and Computer Engineering, Gifu University, 1-1 Yanagido, Gifu 501-1193, Japan.

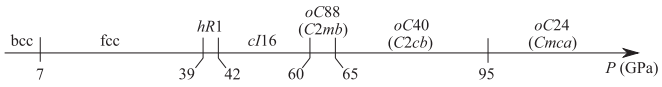

FIG. 1. Schematic of the pressure phase diagram for Li (adopted from Refs. [5,7–10,33]). Transition pressures reported here are from experiments performed at 200 K. The low-temperature phase that appears below 100 K and at ambient pressure (Ref. [37]) is not shown here.

indicating a band gap closure for the range in which the $oC40$ structure is stable. At pressures above 120 GPa and accompanied by the $oC40 \rightarrow oC24$ structural transition, the temperature dependence of resistivity changes from negative to positive, indicating the transition from semiconductor to metal. Although Li retains a metallic character in the $oC24$ structure, its electrical resistivity remains very high (comparable to that of a semimetal such as graphite [29]). Poor electrical conductivity suggests a low electron density of states (e-DOS). Accompanied by the $oC40 \rightarrow oC24$ transition, small but sharp drops in the electrical resistivity vs temperature curves were observed, suggesting a phase transition.

Experiments were performed in BL10XU of SPring-8, using DACs and a cryostat. A monochromatic x-ray beam ($\lambda = 0.4127$ Å) was passed through the sample in a DAC installed inside the cryostat. The diffracted x ray was collected using an imaging plate. The electrical resistance was measured over the duration of the experiment by the standard four-point contact method using an AC-resistance bridge in combination with fine electrodes fabricated on the surface of the diamond anvil. The sample and electrodes were insulated from the Re-metal gasket using an insulation layer made of compressed diamond powder and epoxy mixture. The insulations between sample and gasket, and electrodes and gasket, were confirmed by monitoring electrical connections between them during the experiments. The details of the deposited electrodes and gasket can be found in Ref. [14]. A tiny Li sample was cut from a foil (^{7}Li, 99.95%, Johnson-Matthey) and loaded into a sample chamber drilled through the center of a pre-indented gasket. All steps of sample preparation and pressure cell loading were conducted in an Ar gas atmosphere with oxygen and moisture concentrations of less than 1 ppm. A pressure medium was not used. Samples were compressed at room temperature to a certain pressure below 3 GPa and then cooled to an experimental temperature below 100 K. Pressures were tuned at 50 K for values less than 100 GPa and at 100 K for higher pressures. The shift of the first-order Raman band spectra of the diamond anvil facing the sample was used, along with the calibration proposed in Ref. [30], to estimate pressure. Pressure determination based on diamond Raman vibrations deviates somewhat from the widely used ruby pressure scale [31], by approximately 10 GPa at 70 GPa. The benefit of simultaneous measurements in high-pressure experiments, especially in the Mbar region, is worth noting. When some physical properties are measured in separate experiments, it is not guaranteed that samples are under the exact same pressure, stress, and temperature conditions in their respective environments. In order to demonstrate the relationship between crystal structure and electrical characteristics, simultaneous XRD and electrical resistance measurements on the "same" sample is the most straightforward solution.

Figure 2(a) shows XRD profiles obtained at 50 K. The atomic volumes (V_{atom}) calculated using obtained lattice parameters and electrical resistivity (ρ) at 50 K are plotted as a function of pressure (P) in Fig. 2(b). All of the known high-pressure phases [5,7,10,32,33] were observed: bcc (0–8 GPa) $\rightarrow$ fcc (8–39 GPa) $\rightarrow$ $hR1$ (39–44 GPa) $\rightarrow$ $cI16$ (44–73 GPa) $\rightarrow$ $oC88$ (73–80 GPa) $\rightarrow$ $oC40$ (80–120 GPa) $\rightarrow$ $oC24$ (>120 GPa). It is well known that Li is a very weak x-ray scatterer. In this study, the lattice parameters of the $oC40$ structure between 80 GPa and 110 GPa could not be determined because of the considerably weak and broad XRD signals. The phase boundary at 80 GPa is the point at which XRD signals from $oC88$ vanish. The V_{atom} vs P curve is basically in agreement with previous studies by Guillaume *et al.* [10]. Differences in structural transition pressures between this study and Ref. [10] might be due to the difference in experimental temperatures: 50 K and 90–300 K, respectively.

Figure 2(c) shows the pressure dependence of the ρ and the resistance (R) for Li at 50 K. The value of ρ was calculated from R using the area to length ratio of the Li sample between electrodes measured before loading, for which we used $l \times w \times t$ ($l = 8$ μm, $w = 25$ μm, and $t = 20$ μm). Here, l is the separation between two electrodes for the voltage measurement, w is the width of the sample perpendicular to the current flow, and t is the thickness of the sample. According to the observed V_{atom} vs P relation, the V_{atom} at 137 GPa was approximately 32% of its value under ambient conditions [Fig. 2(b)]. Because visual observations indicated that l and w did not change, we assumed that only t changed by 68% under compression at 137 GPa. Systematic uncertainties in ρ are estimated to be less than 68% up to 137 GPa. Although 68% is a large number, systematic uncertainties allow for the observation of changes in electrical characteristics. The pressure dependence of ρ at pressures below 100 GPa is consistent with our previous experiments performed at 25 K [14]. There is a significant and continuous increase in the value of ρ with applied pressure in the pressure range in which Li is metallic. A decrease in ρ near 40 GPa is attributed to $hR1 \rightarrow cI16$ transitions. Accompanied by the transition from metallic $oC88$ to the semiconducting $oC40$ structure, the value of ρ abruptly increases by more than four orders of magnitude. The value of ρ reaches a maximum of 4×10^4 mΩ cm at approximately 100 GPa, which is comparable to that of a typical semiconductor such as silicon (Si) [34]. Furthermore, it decreases by four orders of magnitude under further compression up to 120 GPa. Regarding the continuous increase in ρ crossing the structural phase boundary between $oC88$ and $oC40$ and its maximum near 100 GPa, the possible contribution by the phase mixing of $oC88$ and $oC40$ cannot be excluded owing to the considerably weak and broad XRD signals in the corresponding pressure range, as mentioned above. At a pressure of 137 GPa in the $oC24$ phase, ρ reaches 8×10^{-1} mΩ cm, which is far from that of typical metals. Several measurements were performed, and reproducible results were obtained for each measurement.

In Fig. 2(d), ρ is plotted as a function of temperature for pressures of 100, 120, and 137 GPa. The ρ vs T curves

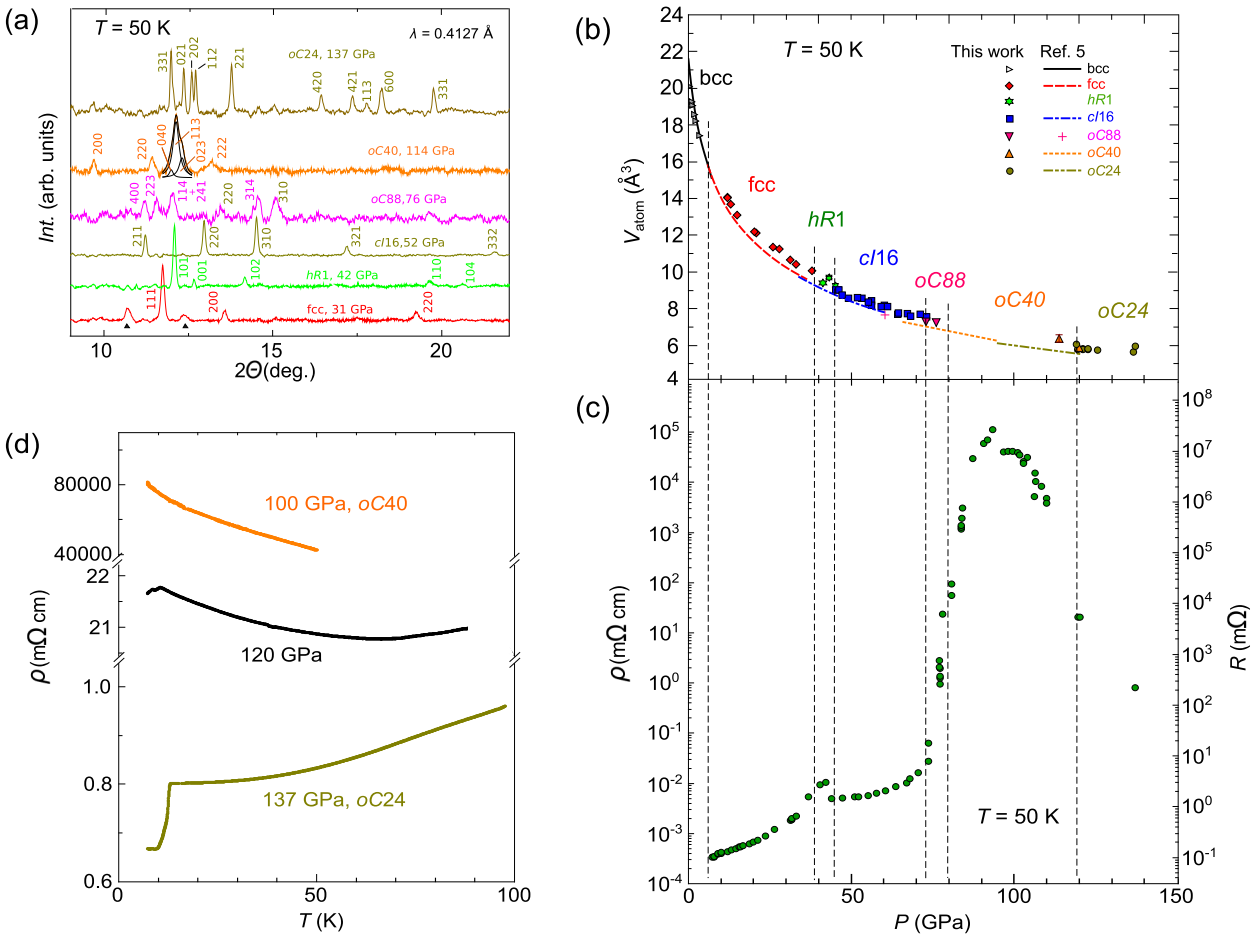

FIG. 2. (Color online) Crystal structure and electrical resistivity of Li under compression. (a) Integrated XRD profiles for Li at 50 K and under different pressures. Solid triangles indicate the reflection from the Pt used in the electrodes. (b) V_{atom} vs P at 50 K with the data obtained in Ref. [5]. Vertical broken lines indicate structural phase boundaries. (c) ρ vs P at 50 K. All experimental data are obtained in pressure loading cycle. (d) ρ vs T for Li at 100, 120, and 137 GPa.

were recorded of both increasing and decreasing temperature, and it was found that the curves taken at each respective process overlap. The data shown in Fig. 2 were taken from the temperature decreasing process. The Li sample under a pressure of 100 GPa in the $oC40$ structure clearly shows semiconducting behavior with a negative $d\rho/dT$ slope. At 120 GPa, where the $oC40 \rightarrow oC24$ transition takes place and the value of V_{atom} is reduced to approximately 27% of that under ambient conditions, the ρ vs T curve shows a negative (positive) slope below (above) 70 K. Although it was not possible to establish the mixed phases of $oC40$ and $oC24$, due to weak XRD signals, the remaining $oC40$ might be attributed to the negative $d\rho/dT$ slope at low temperature. We have found that the upturn of the ρ vs T curve with decreasing temperature is strongly suppressed by applied pressure [Fig. 2(d)]. At a pressure of 137 GPa for a sample that is entirely in the $oC24$ structure, the $d\rho/dT$ slope is positive for temperatures below 100 K. From our experiments, the positive $d\rho/dT$ slope, the ρ value, and the XRD data clearly demonstrate that Li was reverted from a semiconductor back to a metal, accompanied by the $oC40 \rightarrow oC24$ structural transition. The high ρ value at 137 GPa, comparable to that of a semimetal, suggests that $oC24$ is what is termed a "poor metal."

At pressures of 120 and 137 GPa, ρ shows small but clear drops at 10.2 and 12.7 K, respectively [Fig. 2(d)]. These drops in the resistivity were observed reproducibly in two separate experiments where the corresponding pressures were successfully reached. Because no structural transition was confirmed at the corresponding pressure and temperature for the XRD measurement, and the materials in the vicinity of the sample could not have contributed to the measured ρ values, we conclude that these drops in the value of ρ could possibly be attributed to phase transitions. Although zero resistivity was not observed above 7 K, we believe that superconductivity remains a possibility. Here, we call the temperatures where resistivity drops T_x and define them as the temperatures at which ρ deviates from the extrapolated value of the linear section of the ρ vs T curves. At 120 GPa, T_x was defined as the temperature at which ρ starts decreasing.

Our results are summarized in the characteristic phase diagram of Li, which shows the semiconductor phase between the two metallic phases (Fig. 3). T_x and the superconducting transition temperature T_c are plotted as functions of pressure with a visual guide overlaid. In agreement with previous studies [14–18,32], the value of T_c for Li (at ambient pressure, $T_c \leqslant 0.4$ mK [15]) increases significantly at pressures above

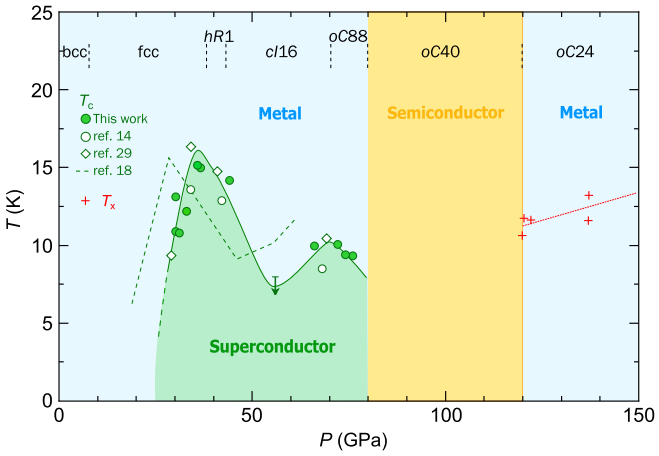

FIG. 3. (Color online) Low-temperature and high-pressure phase diagram of lithium. Here, the T_c data in Refs. [14,29] are taken from electrical resistance measurements using the same measurement method used in this study. The dashed line indicates the data taken under hydrostatic pressure conditions in Ref. [18]. The superconducting transition was not observed above 8 K at 56 GPa (indicated with the downward-pointing arrow). The values of T_x obtained from two separated measurements are plotted as a function of pressure. Vertical broken lines indicate structural phase boundaries.

20 GPa, and its pressure dependence changes according to the crystal structures. T_x increases with applied pressure for $oC24$. Although Li has been theoretically expected to be metallic in $oC24$ [7,23–25] and empirical expectation also suggests that Li becomes a metal again at certain high pressures, there has been no experimental study to verify these predictions. To the best of our knowledge, a pressure-induced re-entrant metallic phase has not been observed previously for any element. With respect to compounds, a similar series of transition has been reported for Fe_3O_4 [35].

In order to discuss the electronic properties of the $oC24$ phase of Li, we compare our experimental observation with theoretical works. Using an *ab initio* density functional calculation, Pickard and Needs have found a very low e-DOS (electron density of states) at Fermi energy E_F for the $oC24$ structure [23]. The re-entrant metallic phase of $oC24$ has also been theoretically predicted to exhibit large interstitial electron density accumulation [7,24,36] due to the high value of the electron localization function (ELF), similar to the case for the semiconducting $oC40$, thereby suggesting a poor conductivity. The present experimental observations support these theoretical predictions on the point of poor electrical conductivity. It is believed that an energy gap of a few meV in the $oC40$ structure is readily decreased by a small atomic volume reduction ($\sim$0.5 Å^3), resulting in a band gap closure and the production of a small number of conduction carriers. If the drops in resistivity at T_x are due to superconducting transitions, the high ELF may play a role in the mediation of valence electrons and the lattice to form Cooper pairs. This would be a direct result of the strong correlation between valence electrons and the ion lattice.

In summary, we have experimentally shown that Li, which is a semiconductor in the $oC40$ structure, reverts to a metallic state, accompanied by the $oC40 \rightarrow oC24$ structural transition, upon further compression. A high ρ value indicates that Li in the $oC24$ structure is a poor metal. Also, some low-temperature phases were found to exist in the re-entrant metallic region. The present study demonstrates the existence of a semiconductor phase between two distinct metallic phases. The compressed light alkali metal Li has been contributing to broadening our understandings of metals as we move towards an increasing degree of compression. The present study provides a basis for further experimental and theoretical investigation of the electronic states of the re-entrant metallic phase of Li, including the origin of drops in resistivity near 10 K and the role of quantum effects. Such studies serve to enhance our understanding of this anomalous yet simple element.

This study was supported by the JSPS, NEXT Program (GR068) and by the Global COE Program, MEXT, Japan. Experiments were performed at BL10XU in SPring-8 (Proposal Nos. 2011B0038 and 2012A0038).

[1] E. Wigner and F. Seitz, Phys. Rev. **43**, 804 (1933).
[2] J. B. Neaton and N. W. Ashcroft, Nature (London) **400**, 141 (1999).
[3] A. Bergara, J. B. Neaton, and N. W. Ashcroft, Phys. Rev. B **62**, 8494 (2000).
[4] A. Rodriguez-Prieto, A. Bergara, V. M. Silkin, and P. M. Echenique, Phys. Rev. B **74**, 172104 (2006).
[5] M. Hanfland, K. Syassen, N. E. Christensen, and D. L. Novikov, Nature (London) **408**, 174 (2000).
[6] B. Rousseau and N. W. Ashcroft, Phys. Rev. Lett. **101**, 046407 (2008).
[7] M. Marqués, M. I McMahon, E. Gregoryanz, M. Hanfland, C. L. Guillaume, C. J. Pickard, G. J. Ackland, and R. J. Nelmes, Phys. Rev. Lett. **106**, 095502 (2011).
[8] J. Lv, Y. Wang, L. Zhu, and Y. Ma, Phys. Rev. Lett. **106**, 015503 (2011).
[9] F. A. Gorelli, S. F. Elatresh, C. L. Guillaume, M. Marqués, G. J. Ackland, M. Santoro, S. A. Bonev, and E. Gregoryanz, Phys. Rev. Lett. **108**, 055501 (2012).
[10] C. L. Guillaume, E. Gregoryanz, O. Degtyareva, M. I. McMahon, M. Hanfland, S. Evans, M. Guthrie, S. V. Sinogeikin, and H.-K. Mao, Nat. Phys. **7**, 211 (2011).
[11] Anne Marie J. Schaeffer, W. B. Talmadge, S. R. Temple, and S. Deemyad, Phys. Rev. Lett. **109**, 185702 (2012).
[12] V. E. Fortov, V. V. Yakushev, K. L. Kagan, I. V. Lomonosov, V. I. Postnov, and T. I. Yakusheva, JETP Lett. **74**, 418 (2001).
[13] M. Bastea and S. Bastea, Phys. Rev. B **65**, 193104 (2002).
[14] T. Matsuoka and K. Shimizu, Nature (London) **458**, 186 (2009).
[15] J. Tuoriniemi, K. Juntunen-Nurmilaukas, J. Uusvuori, E. Pentti, A. Salmela, and A. Sebedash, Nature (London) **447**, 187 (2007).

[16] K. Shimizu, H. Ishikawa, D. Takao, T. Yagi, and K. Amaya, Nature (London) **419**, 597 (2002).
[17] V. V. Struzhkin, M. I. Eremets, W. Gan, H.-K. Mao, and R. J. Hemley, Science **298**, 1213 (2002).
[18] S. Deemyad and J. S. Schilling, Phys. Rev. Lett. **91**, 167001 (2003).
[19] M. Sakata, Y. Nakamoto, K. Shimizu, T. Matsuoka, and Y. Ohishi, Phys. Rev. B **83**, 220512 (2011).
[20] J. J. Hamlin, V. G. Tissen, and J. S. Schilling, Physica C **451**, 82 (2007).
[21] M. Debessai, J. J. Hamlin, and J. S. Schilling, Phys. Rev. B **78**, 064519 (2008).
[22] Y. Ma, M. Eremets, A. R. Oganov, Y. Xie, I. Trojan, S. Medvedev, A. O. Lyakhov, M. Valle, and V. Prakapenka, Nature (London) **458**, 182 (2009).
[23] C. J. Pickard and R. J. Needs, Phys. Rev. Lett. **102**, 146401 (2009).
[24] R. Rousseau, K. Uehara, D. D. Klug, and J. S. Tse, ChemPhysChem **6**, 1703 (2005).
[25] B. Rousseau, Y. Xie, Y. Ma, and A. Bergara, Eur. Phys. J. B **81**, 1 (2011).
[26] N. W. Ashcroft, Phys. Rev. Lett. **21**, 1748 (1968).
[27] C. F. Richardson and N. W. Ashcroft, Phys. Rev. Lett. **78**, 118 (1997).
[28] E. Babaev, A. Sudbø, and N. W. Ashcroft, Nature (London) **431**, 666 (2004).
[29] A. H. Cottrell, *An Introduction to Metallurgy*, 2nd ed. (Maney Publishing, London, 1997).
[30] Y. Akahama and H. Kawamura, J. Appl. Phys. **100**, 043516 (2006).
[31] H. K. Mao, J. Xu, and P. M. Bell, J. Geophys. Res. **91**, 4673 (1986).
[32] T. Matsuoka, S. Onoda, M. Kaneshige, Y. Nakamoto, K. Shimizu, T. Kagayama, and Y. Ohishi, J. Phys. Conf. Ser. **121**, 052003 (2008).
[33] M. Hanfland, I. Loa, K. Syassen, U. Schwarz, and K. Takemura, Sol. Stat. Commun. **112**, 123 (1999).
[34] R. A. Serway and J. W. Jewett, *Principles of Physics*, 2nd ed. (Saunders College Pub, Fort Worth, 1998).
[35] W. M. Xu, G. Yu. Machavariani, G. Kh. Rozenberg, and M. P. Pasternak, Phys. Rev. B **70**, 174106 (2004).
[36] Y. Ma, A. R. Oganov, and Y. Xie, Phys. Rev. B **78**, 014102 (2008).
[37] A. W. Overhauser, Phys. Rev. Lett. **53**, 64 (1984).